International Journal of Advanced Engineering and Technology
ISSN: 2456-7655; Impact Factor: RJIF 5.54
Received: 04-11-2019; Accepted: 06-12-2019; Published: 13-01-2020
www.newengineeringjournal.com
Volume 4; Issue 1; 2020; Page No. 15-19

Modeling of the implantation characteristics of a photovoltaic pump in the village Heremakonon prefecture of Dinguiraye (Republic of Guinea)

Amadou Diarra[1*], Sigguy Ayang[2], Cellou kanté[3], Ansoumane Sakouvogui[4], Mamby Keïta[5]
[1] Department of Mechanical Engineering, Gamal Abdel Nasser University of Conakry, Guinea
[2] Mongo Polytechnic University Institute, Tchad
[3, 4] Energy Department, Higher Institute of Technology of Mamou, Guinea
[5] Department of Physics, Gamal Abdel Nasser University of Conakry, Guinea

Abstract
The database of the Regional Solar Program of the Inter-State Committee for Drought Control in the Sahel using the SP8A7 motor pump covering a panel of 8 villages in Tchad served as a database for the construction of a model mathematical to describe the system. The model was built by highlighting that: The delivery height of a centrifugal pump is a function of the square of the motor speed. This quadratic model was therefore used to establish the dependence between the total head and the flow rate by taking the engine speed as a parameter. The similarity principles were used to assess the new settlement characteristics in Guinea. Highlighting the peculiarities of the two sites, two points of similar operating regime were established. The feasibility of transplanting between the two sites was established by satisfying the criterion of similarity.

Keywords: modeling, characteristics, implantation, photovoltaic

Introduction

Water is at the heart of local, social, environmental and political concerns. Managing this resource both quantitatively and qualitatively has become a major issue. Progress must be made to preserve water and control its sanitary quality. In modern times, water is still at the heart of the news [1].
Access to drinking water is one of the criteria included in the Sustainable Development Goals (SDGs) and contributes greatly to poverty reduction. Access to safe water is indeed an essential condition for health, a basic right and a key component of health protection policies. Access to clean water cuts health-related costs, as 80 % of diseases in developing countries are linked to clean water [2]. Safe drinking water is watering whose microbiological, chemical and physical characteristics comply with the directives of the World Health Organization or national standards concerning the quality of drinking water. Safe drinking water poses no significant risk to a person's health throughout their life. The concept of water scarcity targets them for countries with scarce water resources, which does not necessarily mean that the population suffers from limited access to potable water. Conversely, a population living in a country, with a significant availability of renewable water, does not systematically have safe water [2].
From a scientific point of view, the permanent lack of water has its origin in two main phenomena, namely aridity and desertification. Respectively, the first is natural and the result of low rainfall and spongy soil, while the second depends on Man, who has depleted the soil and exploited the groundwater improperly. This lack of water is irreversible and forces people to take it into account in its land management based on village water programs. Very little of the abundant water on Earth is actually accessible and suitable for human needs. This is particularly true in Africa. On a continent-wide scale, renewable water resources (3931 km³) represent around 9 % of the world's total freshwater resources, in comparison, South America and Asia have the highest proportions, with 28.3 % each, followed by North America with 15.7% and Europe with 14.9 %. Africa is the second driest continent, after Australia, but also the most populous continent, after Asia. Table 1.1 shows that for 2008, the average annual water coverage per capita, continent-wide was 4008 m³, which is well below the world average of 6498 m³ per inhabitant per year [3].
Millions of people in Africa suffer from water scarcity, all year round, water scarcity is not only caused by geography: population growth, rapid urbanization, poor planning and poverty are significant factors [4]. Within the framework of village water supply programs, drilling has increased in recent decades. These boreholes, equipped with hand or foot pumps, satisfied the alarming drinking water needs of the time. They supply less than one cubic meter of water per hour at depths of up to 60 m. This system was well suited to villages with low demography (200 to 500 inhabitants), or around fifty households. The number of towns ranging from 500 to 5000 inhabitants has multiplied rapidly with population growth. This demographic increase requires better adapted systems, closer to urban hydraulics: motor pumps, water tower, distribution network, etc. While these pumping systems are the most suitable solution, their consumption of electrical energy poses enormous problems, given the remoteness of these rural areas from the urban electricity networks, which are themselves in deficit [5]. However, in these areas there is an abundance of solar energy resources which can be excellent alternative solutions for these pumping systems. A double and sustainable solution therefore lies in the use of photovoltaic energy for the supply of drinking water.
For the implementation of these solar energy resources, two photovoltaic pumping systems are possible: the pumping system over the sun and the pumping system with battery. In

one or the other system, photovoltaic pumping, making it possible to obtain significantly higher flow rates, appears to be the option at a lower cost if we compare the investment and operating costs over the entire period. of life of the installations. Solar pumping is therefore the palliative solution between manual village hydraulics and conventional electric motor pumps.
The use of photovoltaic energy provides a sustainable solution to dewatering in rural areas. It is in this context that the member countries of Inter-State Committee to Combat Drought in the Sahel have set up the Regional Solar Program. The sector balance sheet which stands at 113 solar pumps produced in Chad is an eloquent illustration of the success of the Regional Solar Program [6]. Drawing on these results, we considered carrying out the present study of the conditions for setting up the SP8A7 motor pump in a village in the Republic of Guinea.

Material and Method

Material

We want to install the Type SP8A7 photovoltaic pump in the village Heremakonon, in the prefecture of Dinguiraye, Republic of Guinea. The prefecture of Dinguiraye located between 11°18′03 north, 10°43′05 west, with an area of 14,500 km2 and has a population of 210,043 inhabitants (in 2016). We used the SILAB 5.4.1 Console software for the simulation of the model, the Microsoft Excel software for the regression and a database on the Regional Solar Program site.

Method

This study aims to model the characteristics of the SP8A7 motor pump. Also, by the principles of similarity, evaluate the new characteristics of installation of pumps in Guinea.

Hypotheses

The hypotheses for carrying out this study are as follows:

- The pumping system is with the wire of the sun with a pump unit of the submerged monobloc type with alternating current, whose rotation speed is 3300 rpm;
- The pipes are dimensioned for a sufficient diameter so that the pressure losses correspond at most to 10% of the total geometric height with a tank placed at an optimum height estimated at 5 meters;
- In accordance with the current objective of the bodies financing village water supply programs, the water requirement is 20 liters per day per person and an average of the number of inhabitants per family estimated at 10 [7].

Characteristics of the centrifugal pump

From the site of the Regional Solar Program (Inter-State Committee to Combat Drought in the Sahel), with data on solar photovoltaic pumps installed in Sahelian regions of Africa, three representative panels were formed. These panels are based on pump sizing data and network parameters for all sites with the same type of pump [6, 8]. The diagram of the installation model is presented in figure 1 [9].

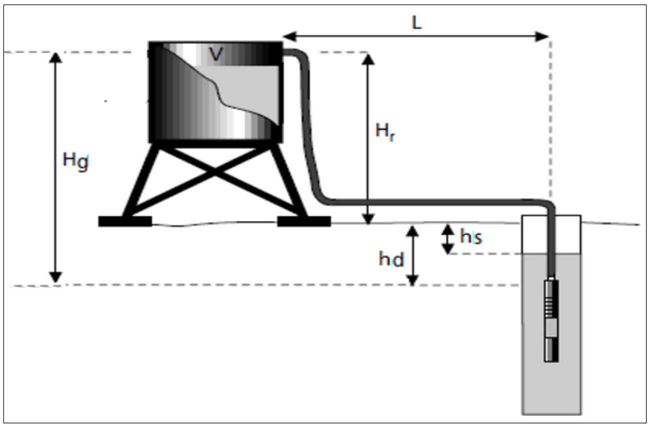

Fig 1: Diagram of the installation model

The model was built by highlighting that, the delivery height of a centrifugal pump is a function of the square of the motor speed. As the Total Manometric Height (HMT) increases, the efficiency of the pump decreases very quickly, the motor should run much faster to provide the same flow [10,11].
This quadratic model was therefore used to establish the dependence between the total head H and the flow Q, taking as a parameter the engine speed (equations 1) [12, 13].

$$\mathrm{H = b.\omega^2 - a.Q^2} \quad (1)$$

Or, ω : Angular velocity (rad/sec); H : Total head (m); Q: Flow rate (liter/min); a, b : Correlation coefficients.
The correlation coefficients (a) and (b) were determined by solving a system of equations $H = f(Q)$. The maximum (H_{max}) and the minimum (H_{min}) corresponding to the maximum and minimum flow rates possible. (equation 2) [14, 15].

$$\begin{cases} H_{max} = b.\omega^2 - a.Q_{vmax}^2 \\ H_{min} = b.\omega^2 - a.Q_{vmin}^2 \end{cases} \quad (2)$$

The characteristic of the hydraulic network is given by a quadratic equation, in which the total head is expressed as a function of the square of the flow (equation 3) [9].

$$H_h = h_S + K_h \cdot Q^2 \quad (3)$$

h_S : Static height; $K_h = \frac{\Delta h}{Q^2}$: Hydraulic constant which takes into account linear and singular head losses. These losses $\Delta h = K_h \cdot Q^2$ are a function of the length of the pipes, their diameter and the flow rate (Q) of the pump and are expressed in meters of water. They correspond at most to 10% of the total geometric height [9].
The operating point of the model is given by the intersection of the network curve with the pump curve. For a given rotation speed (3300 rpm), the operating point must check the equality ($H = H_h$).

$$Q_{vm} = \sqrt{\frac{b\cdot\omega^2 - h_0}{K_h + a}} \quad (4)$$

$$H_m = b.\omega^2 - a.Q_{vm}^2 \quad (5)$$

To obtain other characteristics of the same pump corresponding to rotational speeds $n = 3000\ tr/min$ and $3600\ tr/min$, we used the similarity relation (equation 6).

$$\frac{H_m}{H} = \frac{n_m^2}{n^2} = \frac{Q_{vm}^2}{Q_v^2} \qquad (6)$$

At variable speed, the calculation aims to determine the characteristic required to reach the various operating points of the system using the speeds as a control variable.
From equation 6, it was easy for us to establish the equation of the parable of the operating regimes which pass through the origin of the coordinates *H = f (Q)*.

$$\frac{H_m}{Q_{vm}^2} = \frac{H}{Q_v^2} = Const \qquad (7)$$

Hence, for a series of similar operating regimes, we have equations 8 and 9.

$$H_1 = Cont_1 \cdot Q_v^2 \qquad (8)$$

For another series:

$$H_2 = Cont_2 \cdot Q_v^2 \qquad (9)$$

The daily flow (*Qv = 24.2* m^3/d) is calculated by the conventional method, which is the product between the number of families (121), the number person per family (10) and the daily need for water (20 liters per person).
Knowing this flow, the new static (h_S) height and the dynamic (h_d) level are by the relations of similarity (equation 10 and 11).

$$h_S = f(Q_v) = \left(\frac{Q_v}{Q_{vm}}\right)^2 \cdot h_{Sm} \qquad (10)$$

$$h_d = f(Q_v) = \left(\frac{Q_v}{Q_{vm}}\right)^2 \cdot h_{dm} \qquad (11)$$

The corresponding total head height created by the pump unit was also evaluated by the classical method (equation 12) [9].

$$H_{MT} = f(Q_v) = 1{,}1 \cdot (h_d + H_r) \qquad (12)$$

The new characteristic of the network is calculated by equation 13.

$$H_h = f(Q_v) = h_S + K_h \cdot Q_v^2 \qquad (13)$$

For a new characteristic of the network corresponding to the reality of the new site, the new operating point must verify the equality of equation 14.

$$h_0 + K_h \cdot Q_v^2 = 1{,}1 \cdot (h_d + H_r) \qquad (14)$$

Hence the flow rate and the Total Manometric Height are given respectively by equations 15 and 16.

$$Q_v = \sqrt{\frac{1{,}1 \cdot (h_d + H_r) - h_S}{K_h}} \qquad (15)$$

$$H_{MT} = H_h = h_S + K_h \cdot Q_v^2 \qquad (16)$$

Given that for the same SP8A7 pump rotating at speed (3300 rpm) in two operating regimes, the condition for transplanting between two sites must satisfy the criterion of similarity on the constancy of the angular speed coefficient (equation 17) [16, 17].

$$\left(\omega \cdot \frac{Q_v^{1/2}}{(gH_{MT})^{3/4}}\right)_m = \left(\omega \cdot \frac{Q_v^{1/2}}{(gH_{MT})^{3/4}}\right)_n = C_\omega = Cte \qquad (17)$$

Results and Discussion

Results

The results (the characteristic curves and points of regime of the model, the parables of similarity of the operating regimes) obtained are presented by in figures. 2, 3 and 4.
The flow-height curves *(H = f (Q))* (figure 2), express the variations of the different total head heights as a function of the flows. They express the performance of the pump, for a given speed of rotation. Because the water is pumped from a borehole to an upper reservoir, that is to say that the static height is different from zero, the characteristic of the network is therefore a second-degree parabola not passing through the origin of coordinates.

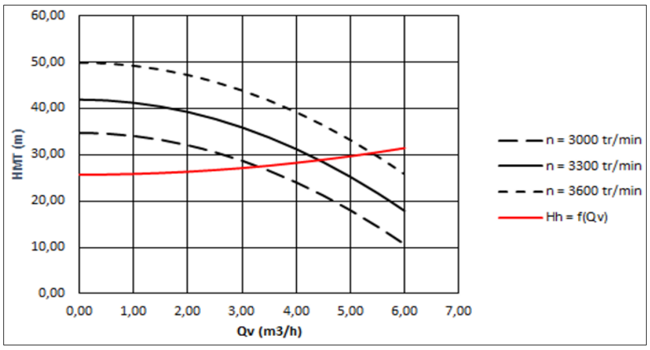

Fig 2: Characteristic curves and regime points of the model

Figures 3 and 4 illustrate the dimensionless features of the model. The different parables of similarity which pass through the origin of the coordinates, cut the operating curves at the respective speed points.

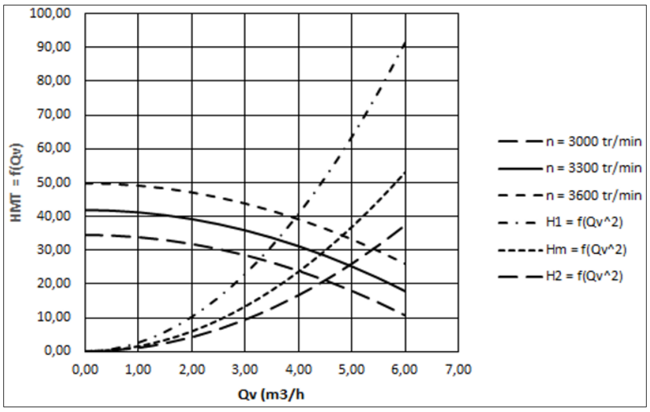

Fig 3: Parables of similarity of operating regimes

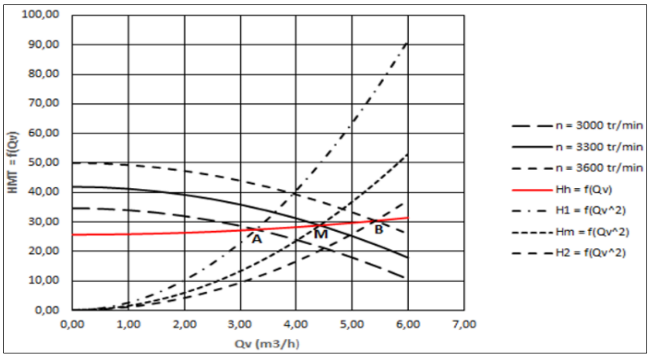

Fig 4: Curve of networks, similarity dishes and points of operating regime

Discussion

From Figure 2, (Q_{vm}) and (H_m) characterize the different points of the operating regime of the model. The numerical values calculated for these points as a function of the speeds of rotation are respectively: for n1 = 3000 rpm, we have ($Q_{vm} = 3.29\ m^3/h$ and $H_m = 27.42\ m$), for $n_m = 3300\ rpm$, we have ($Q_{vm} = 4.43\ m^3/h$ and $H_m = 28.83m$) and for $n_2 = 3600\ rpm$ we have ($Q_{vm} = 5.41\ m^3/h$ and $H_m = 30.37m$). These characteristics of the pump show the evolution of the loss of its capacity at total head when its flow increases. Figure 3 shows that the points which correspond to similar operating regimes are arranged on second degree parabolas which pass through the origin of the coordinates.

By highlighting the operating points, it has been illustrated that these parabolas intersect the characteristic curves of the pump at respective operating points (figure 3). So, to adjust the characteristics of the pump by the method of variation of the rotation speed, the operating points must follow the similarity curves as the characteristic curve of the pump increases or decreases. With an appropriate increase or decrease in the speed curve ($n = 3300\ rpm$), the operating point should coincide with the point of intersection when the two curves are superimposed (Figure 4).

From figure 4, we see that the characteristic curve of the network does not pass through the origin of the coordinates, the variation of the rotation speed of $n_m = 3300rpm$, $n_1 = 3000rpm$, $n_2 = 3600rpm$, this causes the speed point to move from M to A and B respectively. It is further noted that the similarity curve which passes through the nominal operating point of the pump at 3300 rpm crosses the two other curves of the pump at *3000 rpm* and at *3600 rpm* at any points.

Thus, on the installation site, the new speed point at nominal speed (3300 rpm) is characterized by $Q_m = 9.85m^3/h$ and $H_m = 49.24m$. The feasibility of transplanting between the two sites is established by satisfying the criterion of similarity on the constancy of the angular speed coefficient [16, 17] between the two points of speed at nominal speed: $C_\omega = 9746.10^{-7} = Constant$.

Conclusion

In the present study, we have succeeded in developing the characteristics of the model motor pump as well as the adjustment range of these characteristics if the rotation speed goes from its nominal value (3300 rpm) to a lower value (3000 rpm). or at a higher value (3600 rpm). The parables of similar regimes have been drawn for this purpose. The transplant study took into account three constraints (the need to operate the motor pump with the same rotation speed, the constraint of satisfying a flow rate imposed by the new site and the constraint of satisfying a total head corresponding to the flow imposed by the new site. Highlighting the peculiarities of the two sites, two points of similar operating regime were established. The feasibility of transplanting between the two sites was established by satisfying the criterion of similarity on the constancy of the speed coefficient angular.

References

1. Rapport de situation sur l'application des approches intégrées de la gestion des ressources en eau en Afrique, 2012, 110p.
2. OMS/UNICEF, Organisation Mondiale de la Santé et UNICEF. Progress on Sanitation and Drinking-Water: Update, 2013.
3. FAO. Food Security Statistics. Food and Agriculture Organization of the United Nations, 2010,
4. Afrique, Atlas de l'Eau, United Nations Environment Programme, Publication Numéro: DEW/1249/NA, ISBN: 978-92-807-3205-4. 2010, 325 p.
5. SCE - Memoris – CREPA, Rapport de diagnostic sur l'état des lieux de la situation existante. Etude sur l'eau et l'assainissement à Kindia, Guinée, 2009, 159 p.
6. IED, « La place du PRS dans la stratégie globale du MDP », Rapport final, 2008, 97p.
7. Louazene ML, Korichi D, Azoui B. Dimensionnement d'un Système de Pompage Photovoltaïque Application sur le Site de Ouargla. The International Conference on Electronics & Oil: From Theory to applications March 05-06, 2013. Ouargla, Algeria, 5 p.
8. Mohamed Lakhdar Louazene, Contribution à l'optimisation des systèmes photovoltaïques utilisés pour l'irrigation dans les zones sahariennes – Application zone de Ouargla. Thèse de Doctorat en Sciences Université El Hadj Lakhdar- Batna, Algérie, 2015, 128 p.
9. Jimmy Royer, Thomas Djiako, Eric Schiller, Bocar Sada Sy; Le pompage photovoltaïque: manuel de cours à l'intention des ingénieurs et des techniciens; ISBN 2-89481-006-7, Québec, 1998, 254p.
10. Sumit K, Gupta M, Rizwan Khan, Kaushar Jahan. Modeling, Analysis and Control of Solar Water Pumping System, Impending Power Demand and Innovative Energy Paths - ISBN: 978-93-83083-84-8, 2015, 356-363.
11. Lei Xie, Wei Deng, Research on water output optimization of photovoltaic pumping, 5th International Conference on Sustainable Energy and Environment Engineering (ICSEEE) Advances in Engineering Research, volume 63 system, 2016, pp. 415-42.
12. Bessem M. Abdelghani, Modélisation et simulation d'un pompage photovoltaïque, Mémoire de Master 2, Badji Mokhtar- Annaba University, 76p.
13. Chiter Lamri, Modélisation et simulation d'un système de pompage solaire à base d'un moteur asynchrone monophasé, Mémoire de Magister, Université de Batna, Algérie, 2012, 73p.
14. Zarour Laid. Etude technique d'un système hybride Photovoltaïque-Eolienne hors réseau, Thèse doctorat, Université Constantine, 2010.

15. Muñoz J, Carrillo JM, Martínez-Moreno F, Carrasco LM, Narvarte L. Modeling and simulation of large PV pumping systems, Presented at the 31st European Photovoltaic Solar Energy Conference and Exhibition DOI: 10.4229/EUPVSEC20152015-6BV.5.42, 2016, 12p.
16. Michel Rapinat, Paul Tanini, Pièrre Roussel; Les Stations de Pompage d'eau – 6èmme édition, Travaux de la commission distribution de l'eau de l'ASTEE; TEC – Paris.
17. Hydro-Québec, Guide technique - Systèmes de pompage Les économies d'énergie électrique dans les systèmes de pompage, Québec, 1993, P94.